

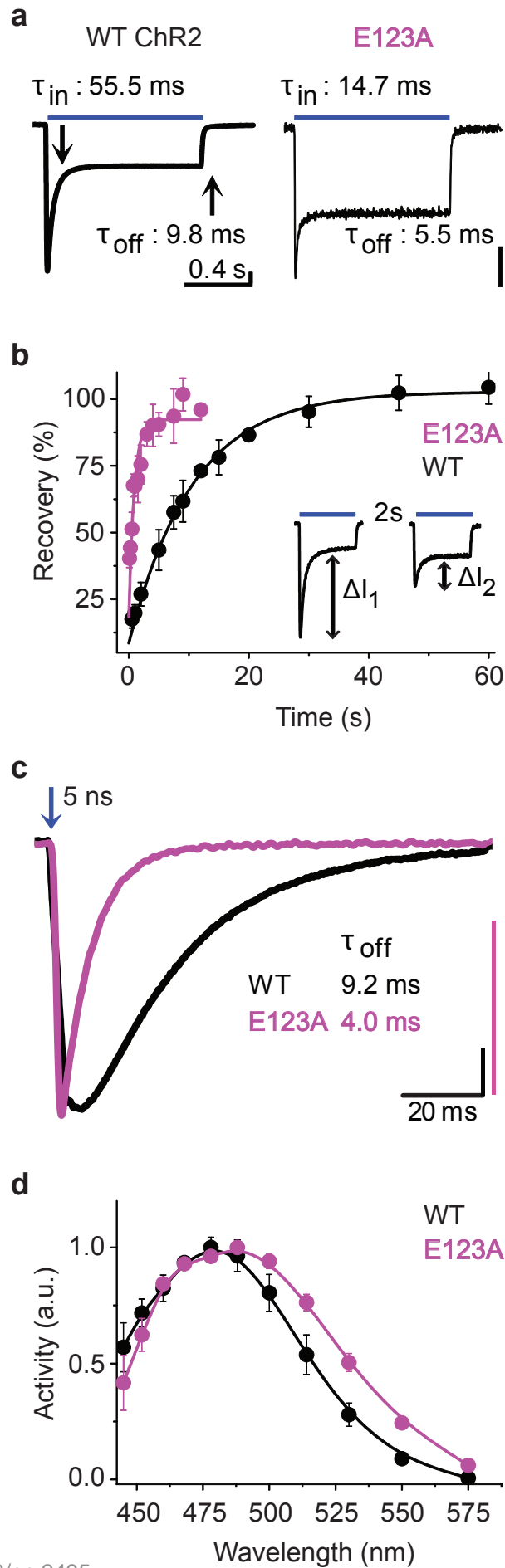
ONLINE SUPPLEMENTARY MATERIAL

Ultrafast optogenetic control

Lisa A. Gunaydin, Ofer Yizhar, André Berndt, Vikaas S. Sohal,
Karl Deisseroth and Peter Hegemann

Correspondence and requests for materials should be addressed to
P.H (hegemape@rz.hu-berlin.de) or K.D. (deissero@stanford.edu).

Supplementary Figure 1. Characterization of an alternative fast mutant: E123A.

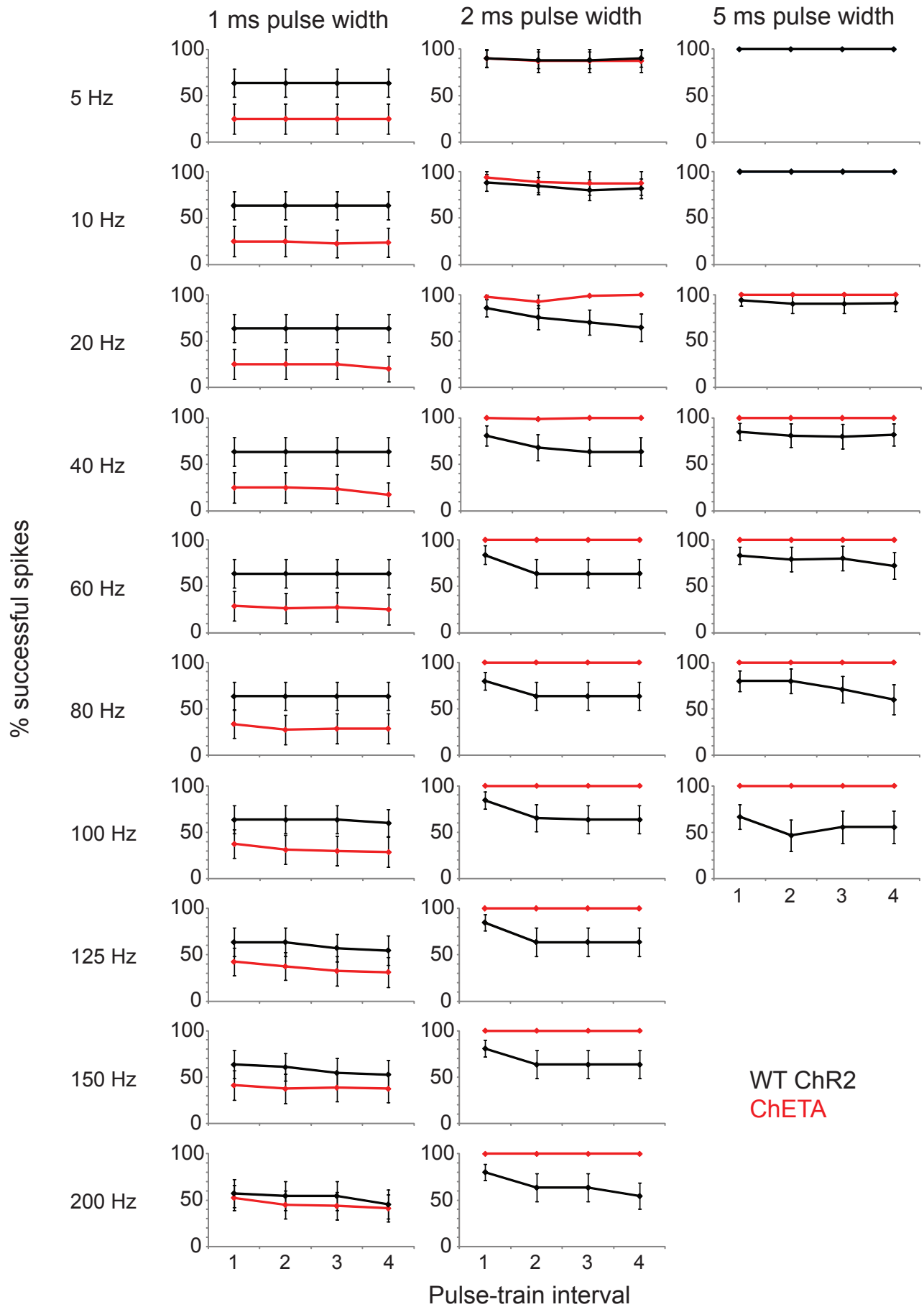


Supplementary Figure 1:

Characterization of an alternative fast mutant: E123A.

(a) Voltage clamp recordings of WT ChR2 and E123A in *Xenopus* oocytes under stimulation with a 1 s light pulse (blue bars, $500 \text{ nm} \pm 25$, 50 mW/cm^2) at -100 mV and 100 mM NaCl in the external solution (pH 7.5). τ -values characterize the mono-exponential transition from peak to stationary currents (τ_{in}) and current kinetics (τ_{off}) after the light was switched off. $\tau_{\text{off}} = 9.8 \pm 1.3 \text{ ms}$ for WT ($n = 10$) and $\tau_{\text{off}} = 6.2 \pm 1.3 \text{ ms}$ for E123A ($n = 11$; $p < 0.005$). Vertical black bars: 10 nA . (b) Recovery of peak current in WT ChR2 and E123A upon stimulation with a second light pulse after a variable dark period, recorded in oocytes. Inset shows the peak recovery of WT ChR2 after 2s in darkness at -75 mV in standard solution (100 mM NaCl , pH 7.5). The ratio of ΔI_2 to ΔI_1 yields the recovery in percent. Values for WT ChR2 (black circles) and E123A (pink circles) are plotted versus the dark interval between the two flashes; data points were fit by a mono-exponential decay (colored lines). Peak recovery was $\tau = 10.7 \pm 0.8 \text{ s}$ for WT ($n = 15$) and $\tau = 0.9 \pm 0.2 \text{ s}$ for E123A ($n = 4$; $p < 0.005$). (c) Oocyte current recordings; excitation delivered with a 5 nanosecond laser flash (470 nm , 0.5 mW/cm^2 , blue arrow) at -100 mV . Photocurrent decay was fitted mono-exponentially with τ -values shown for WT ChR2 (black) and E123A (pink), and traces were normalized to highlight differences in decay kinetics. Off kinetics were $\tau = 9.2 \pm 1.3 \text{ ms}$ for WT ($n = 9$) and $4.0 \pm 0.2 \text{ ms}$ for E123A ($n = 11$; $p < 0.005$). Flash-to-peak current times were $t_p = 2.4 \pm 0.3 \text{ ms}$ for WT ($n = 9$) and $t_p = 0.8 \pm 0.1 \text{ ms}$ for E123A ($n = 11$; $p < 0.005$). Vertical bars correspond to 2.5 nA (WT: black; E123A: pink). (d) The action spectrum of E123A (pink, $n = 3$) is shown in comparison with spectrum of WT ChR2 (black, $n = 6$). Current amplitudes were measured at the different wavelengths, normalized to respective maximum values, and corrected for fluctuations of flash intensity.

Supplementary Figure 2. Temporal stationarity during extended trains.



Supplementary Figure 2:

Temporal stationarity during extended trains.

The percentage of successful spikes is plotted over time for WT ChR2 and ChETA, across a range of light pulse frequency and light pulse width. Note the deterioration over time of WT ChR2 performance in following light pulses. In contrast, the performance of ChETA (in addition to showing improved efficacy at high frequencies for >1 ms pulse width) was temporally stationary, in that performance in response to later light flashes was indistinguishable from that for earlier light flashes in the train, across all conditions. Trains of 40 light pulses were delivered, and spike responses were grouped into four intervals corresponding to successive blocks of 10 light pulses (interval 1 = light pulses 1-10, interval 2 = light pulses 11-20, interval 3 = light pulses 21-30, interval 4 = light pulses 31-40).